SUPPLEMENTAL MATERIAL 2

to

Probing the low-temperature chemistry of di-*n*-butyl ether: Detection of previously unobserved intermediates

Luc-Sy Tran[1,2,3,*], Julia Wullenkord[3], Yuyang Li[4], Olivier Herbinet[2], Meirong Zeng[4], Fei Qi[4], Katharina Kohse-Höinghaus[3], Frédérique Battin-Leclerc[2]

[1] *Physicochimie des Processus de Combustion et de l'Atmosphère (PC2A), CNRS, Université de Lille, F-59000 Lille, France*

[2] *Laboratoire Réactions et Génie des Procédés (LRGP), CNRS, Université de Lorraine, ENSIC, 1, rue Grandville, BP 20451, 54001 Nancy Cedex, France*

[3] *Department of Chemistry, Bielefeld University, Universitätsstraße 25, D-33615 Bielefeld, Germany*

[4] *School of Mechanical Engineering, Shanghai Jiao Tong University (SJTU), Shanghai 200240, PR China*

* Corresponding author: Dr. Luc-Sy Tran
Physicochimie des Processus de Combustion et de l'Atmosphère (PC2A),
CNRS, Université de Lille, F-59000 Lille, France
E-mail: luc-sy.tran@univ-lille.fr

Material presented in this Supplement:

Fig. S1 Comparison of data obtained in the GC and PI-MBMS experiments for DBE and an exemplar intermediate (nC_3H_7CHO). Good agreement between two experiments ensures a similar chemical behavior in the two used JSRs.

Fig. S2 Example of the principle of the used nomenclature for species in DBE destruction pathway, adopted from Ref [1].

Fig. S3 PIE curve at 500 K from the JSR-PI-MBMS experiment for *m/z* 76. The inset shows the same PIE curve, multiplied by 10, in the energy range of 9-10 eV, to indicate potential contributions below 9.5 eV.

Fig. S4 Comparison of the normalized signal profiles of $C_4H_8O_2$ (*m/z* 88, corresponding to butanoic acid) for the three experimental setups.

Fig. S5 Examples of fragmentation rules used to explain the mass spectra from GC-MS and thus to identify the $C_8H_{16}O_2$ cyclic isomers: C_4OC_4Oa-2 (a), C_4OC_4Oa-3 (b), and C_4OC_4Oa-d (c).

Fig. S6. PIE curves at 500 K from the JSR-PI-MBMS experiment for *m/z* 190 and 208.

Comparison of the experiments and the predictions from the models of Thion *et al.* [1] and Cai *et al*. [2] (Figs. S6-S12). Species presented already in the main paper are not included in these figures.

Fig. S7 Comparison of the experimental data and the Thion [1] and Cai [2] models for the main species. Left panel: JSR. Right panel: PFR.

Fig. S8 Comparison of the experimental data and the Thion [1] and Cai [2] models for selected C_1 intermediate species. Left panel: JSR. Right panel: PFR.

Fig. S9 Comparison of the experimental data and the Thion [1] and Cai [2] models for selected C_2 intermediate species. Left panel: JSR. Right panel: PFR.

Fig. S10 Comparison of the experimental data and the Thion [1] and Cai [2] models for selected C_3 intermediate species. Left panel: JSR. Right panel: PFR.

Fig. S11 Comparison of the experimental data and the Thion [1] and Cai [2] models for additional C_3 intermediate species. Left panel: JSR. Right panel: PFR.

Fig. S12 Comparison of the experimental data and the Thion [1] and Cai [2] models for selected C_4 intermediate species. Left panel: JSR. Right panel: PFR.

Fig. S13 Comparison of the experimental data and the Thion [1] and Cai [2] models for selected C_8 intermediate species. Left panel: JSR. Right panel: PFR.

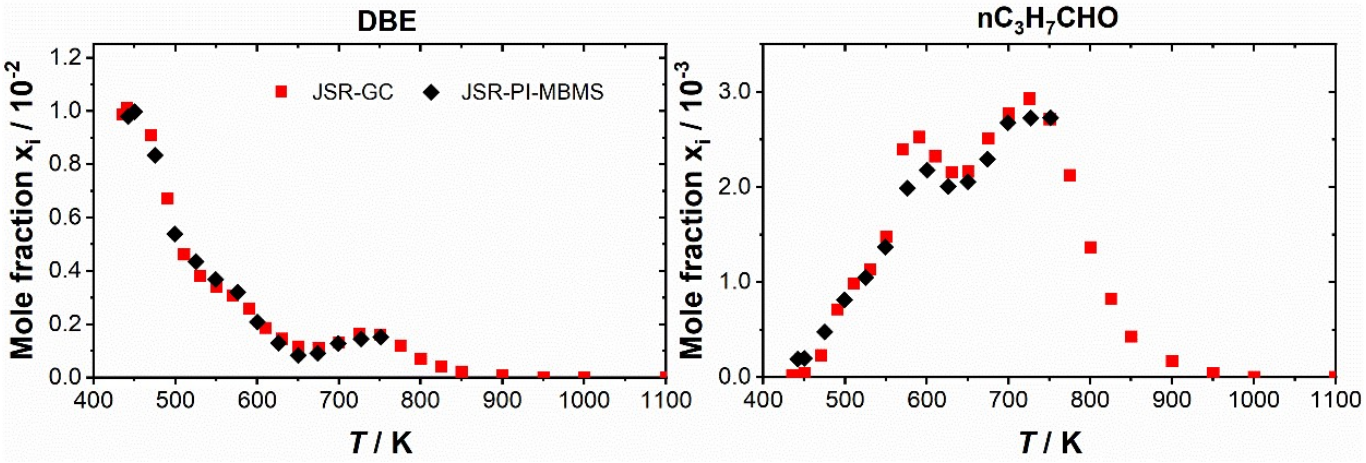

Fig. S1. Comparison of data obtained in the GC and PI-MBMS experiments for DBE and an exemplary intermediate (nC_3H_7CHO). Good agreement between two experiments ensures a similar chemical behavior in the two used JSRs.

The nomenclature of first decomposition products was adopted from the model of Thion et al. [1]. Figure S2 exemplarily presents this principle. A C_4H_x carbon chain is replaced by C_4 if the species' name gets too long. The carbon chain of DBE is labeled numerically (i.e. 1, 2, 3, 4) starting with the carbon at the vicinity of the oxygen atom, while if radical sites being located in the opposite carbon chain, they are denoted alphabetically (i.e., a, b, c, d) starting with the carbon at the vicinity of the oxygen atom. In this way, the radical resulting from the H-abstraction reaction on carbon "a" of DBE ($C_4H_9OC_4H_9$) is therefore called "$C_4H_9OC_4H_8$-a", and "a" is then involved in the subsequent species resulting from the reactions of this radical. When a new radical site is formed, the corresponding label of this radical site is added in the name. For example, a species resulting from an isomerization at carbon "2" of the $C_4OC_4H_8OO$-a radical is named as C_4OC_4-aO_2H-2. "a" and "2" are then involved in their subsequent products, e.g. C_4OC_4Oa-2.

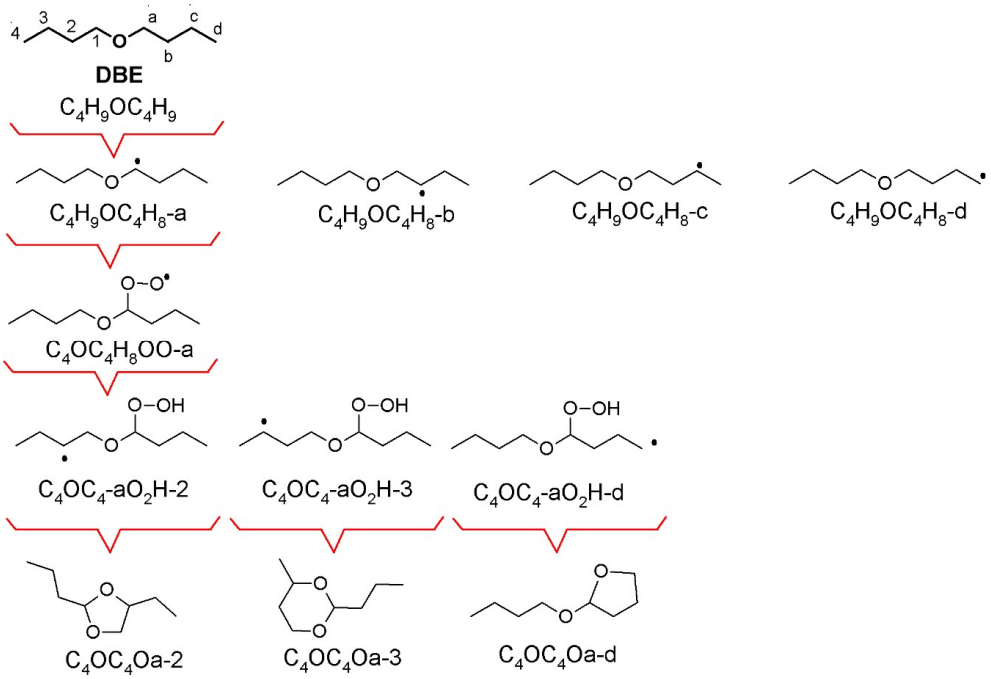

Fig. S2. Example of the principle of the used nomenclature for species in DBE-destruction species, adopted from Ref [1].

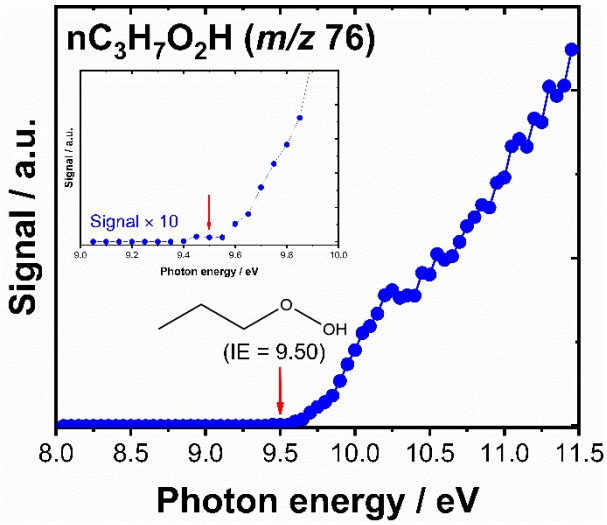

Fig. S3. PIE curve at 500 K from the JSR-PI-MBMS experiment for *m/z* 76. The inset shows the same PIE curve, multiplied by 10, in the energy range of 9-10 eV, to indicate potential contributions below 9.5 eV.

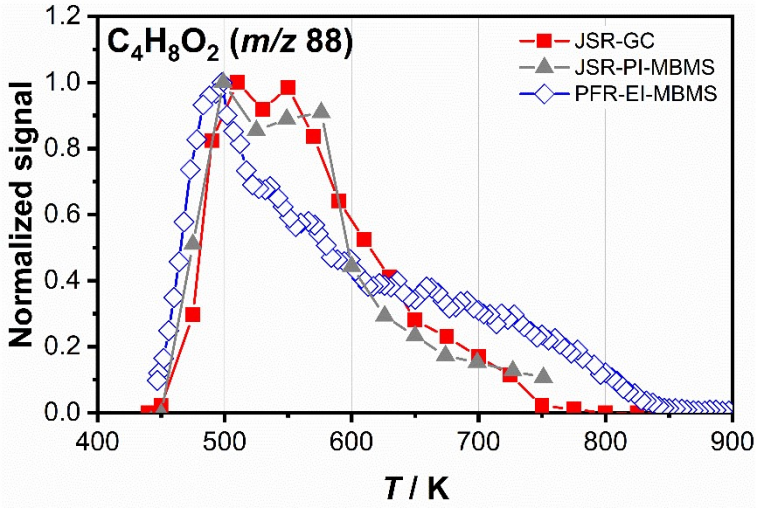

Fig. S4. Comparison of the normalized signal profiles of $C_4H_8O_2$ (*m/z* 88, corresponding to butanoic acid) for the three experimental setups.

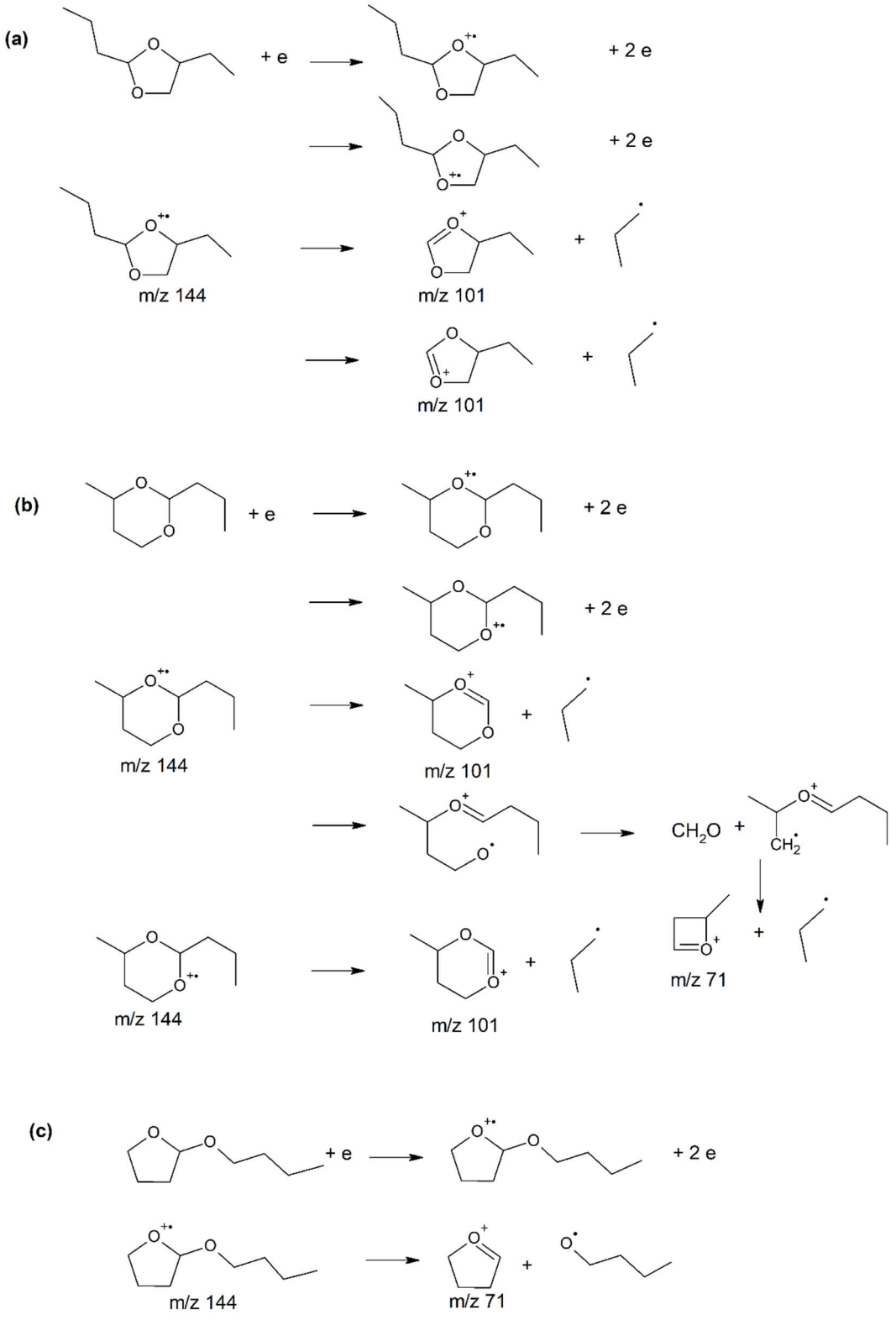

Fig. S5. Examples of fragmentation rules used to explain the mass spectra from GC-MS and thus to identify the $C_8H_{16}O_2$ cyclic isomers: C_4OC_4Oa-2 **(a)**, C_4OC_4Oa-3 **(b)**, and C_4OC_4Oa-d **(c)**.

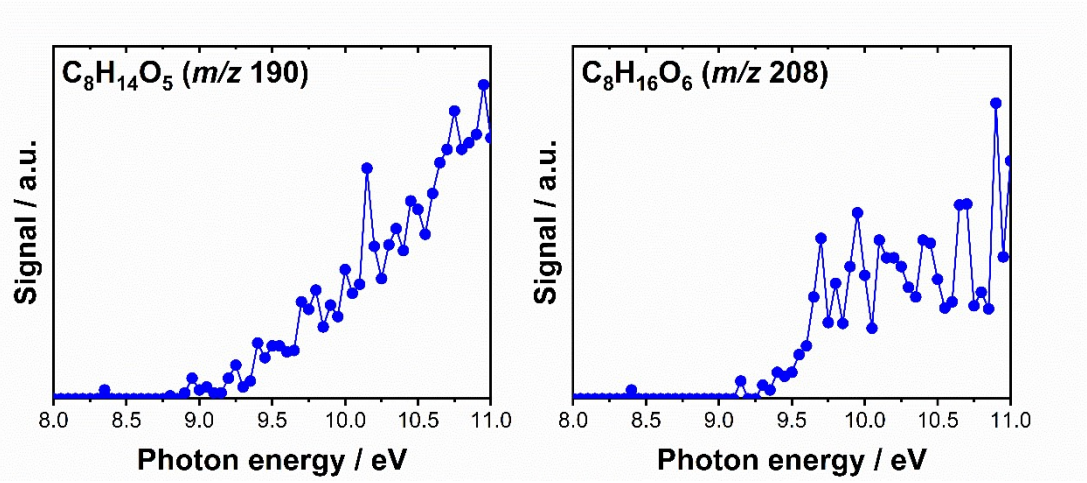

Fig. S6. PIE curves at 500 K from the JSR-PI-MBMS experiment for *m/z* 190 and 208.

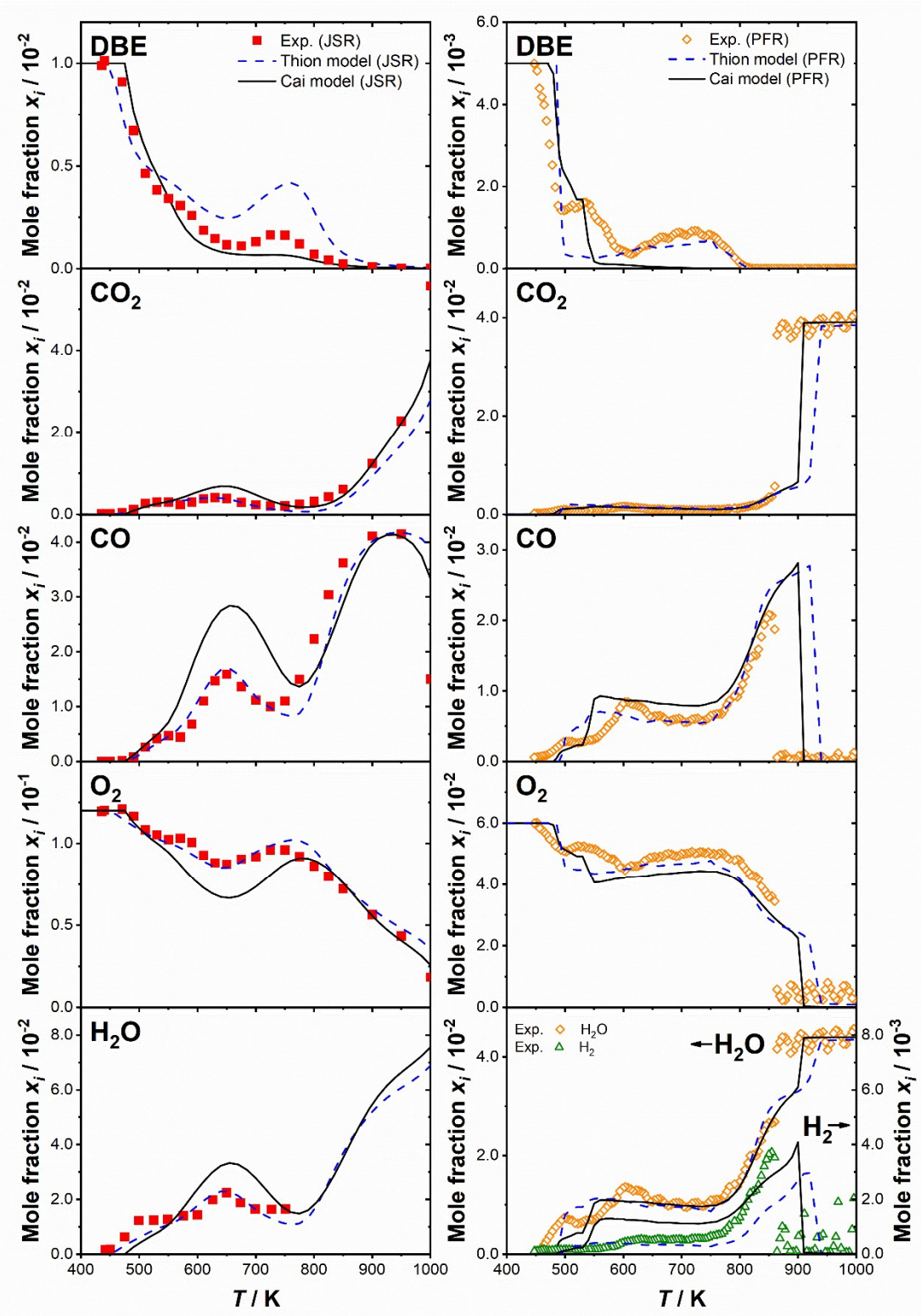

Fig. S7. Comparison of the experimental data and the Thion [1] and Cai [2] model for the main species. **Left panel:** JSR. **Right panel:** PFR.

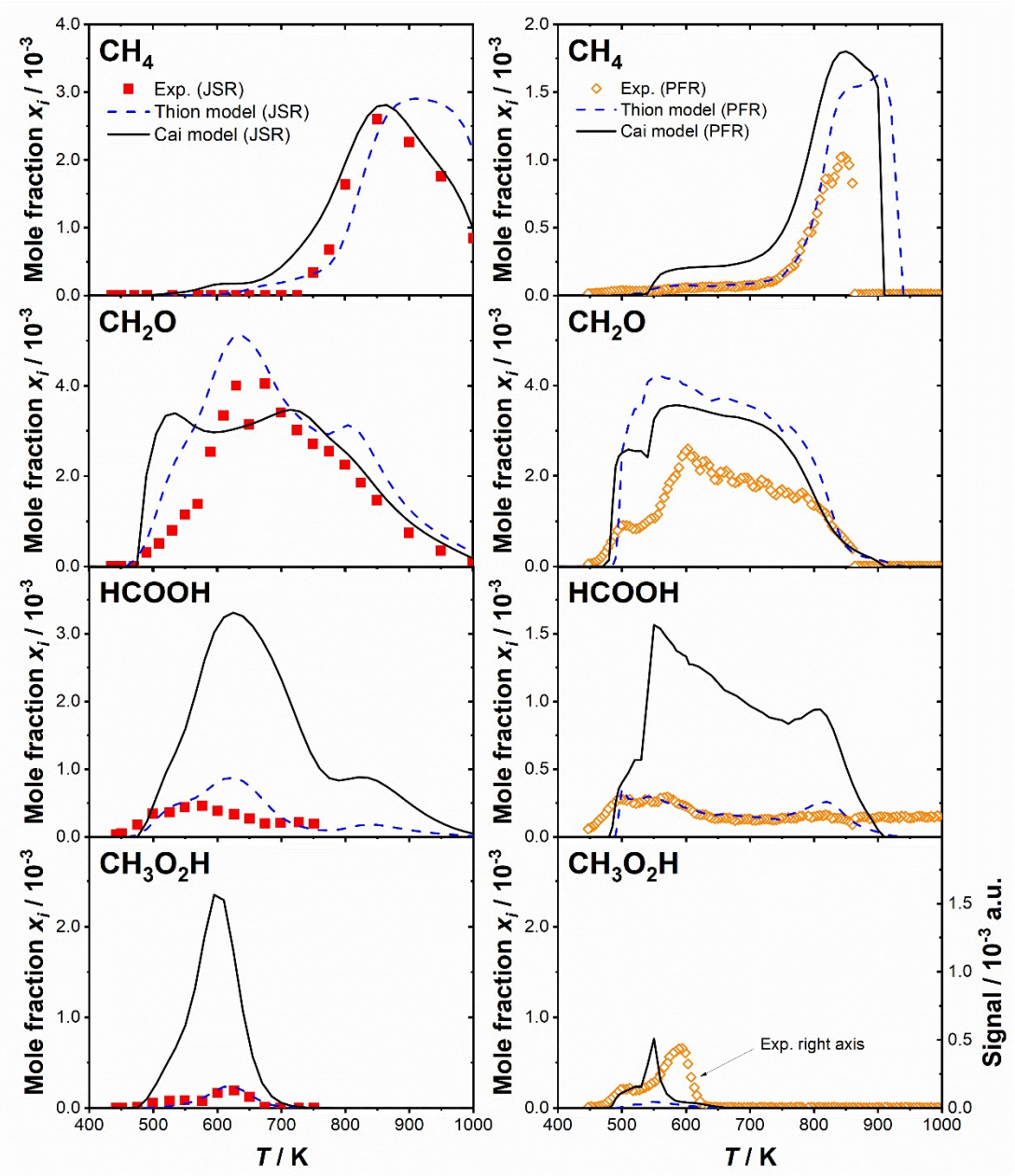

Fig. S8. Comparison of the experimental data and the Thion [1] and Cai [2] model for selected C_1 intermediate species. **Left panel:** JSR. **Right panel:** PFR.

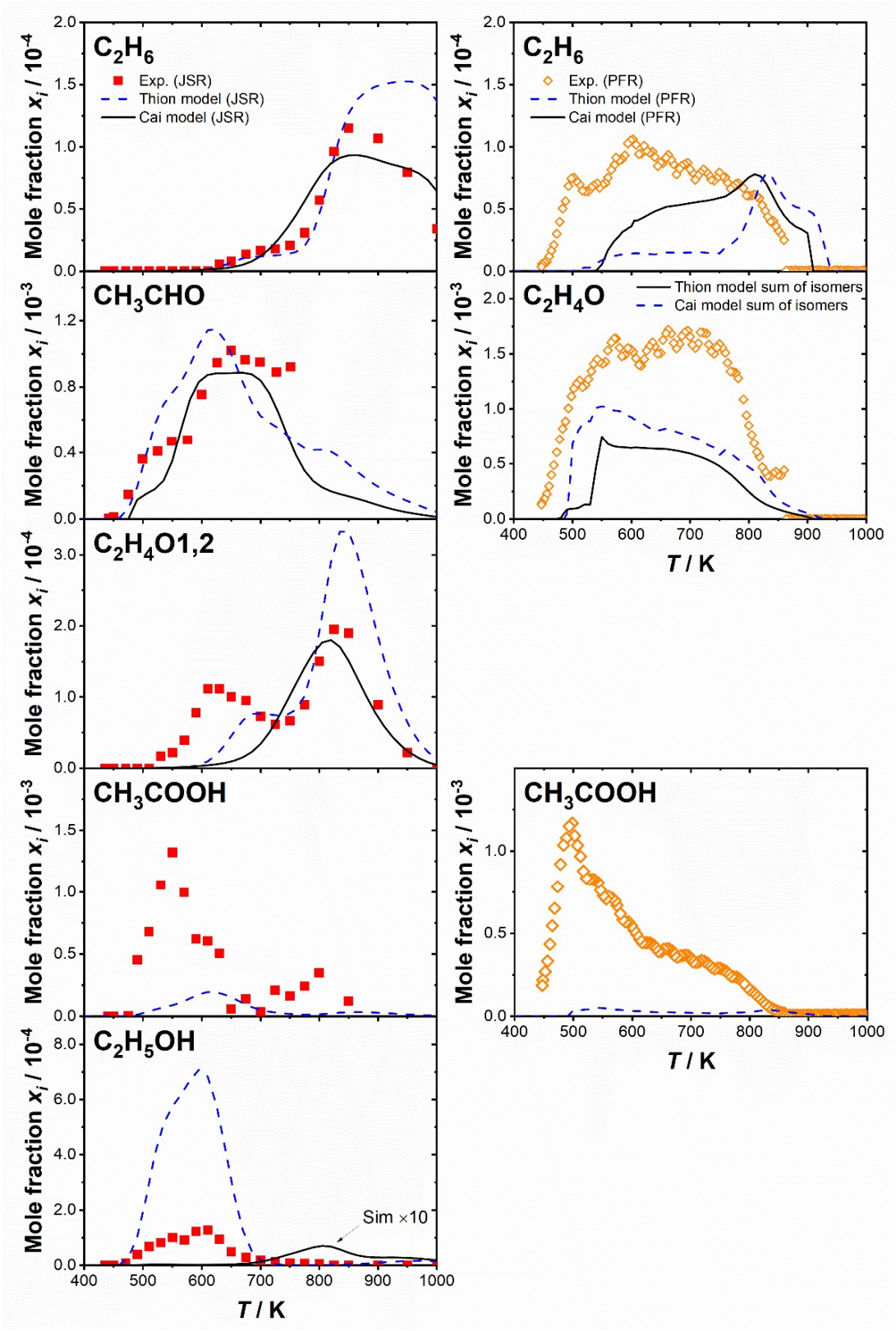

Fig. S9. Comparison of the experimental data and the Thion [1] and Cai [2] model for selected C_2 intermediate species. **Left panel:** JSR. **Right panel:** PFR.

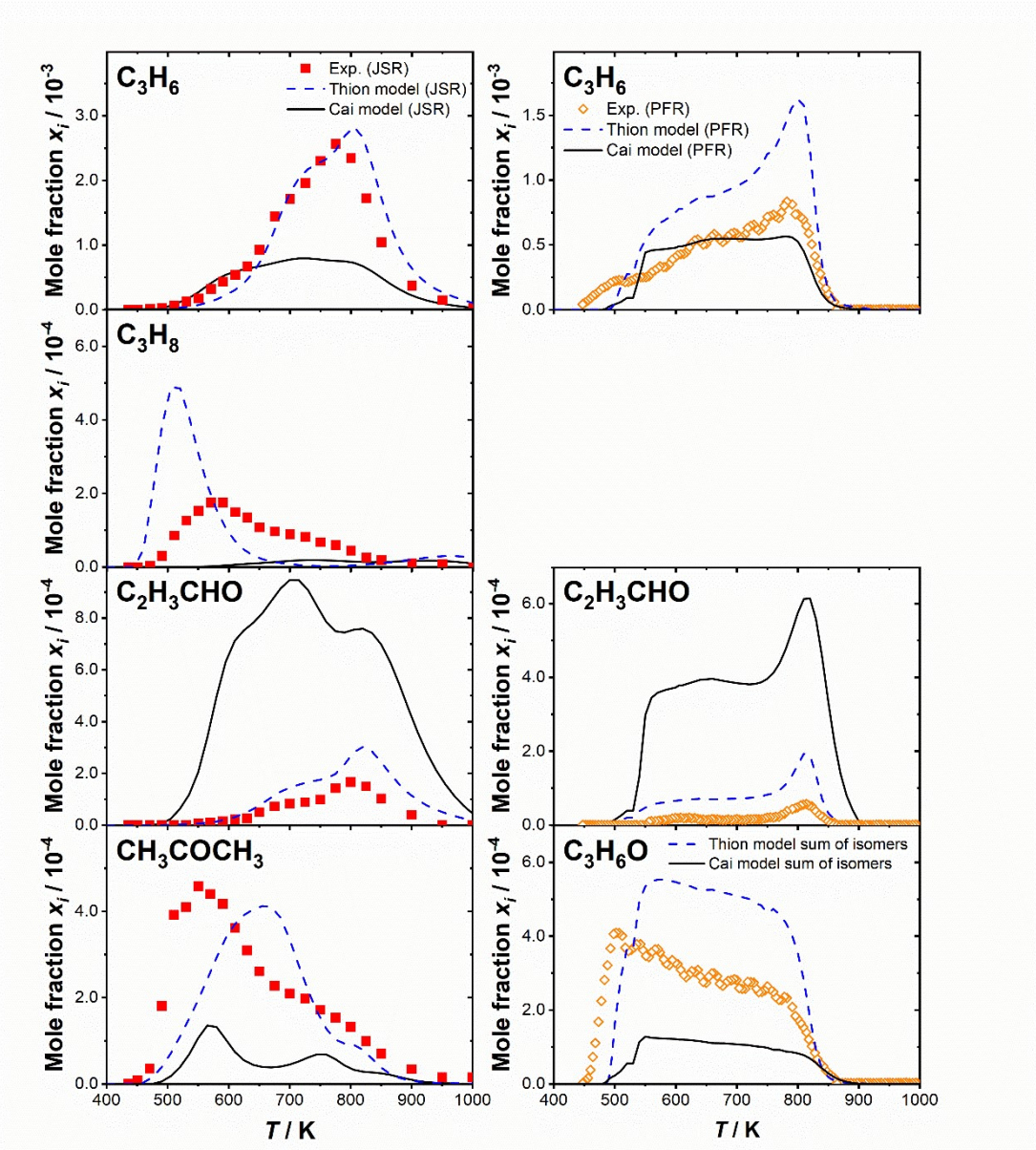

Fig. S10. Comparison of the experimental data and the Thion [1] and Cai [2] model for selected C_3 intermediate species. **Left panel:** JSR. **Right panel:** PFR.

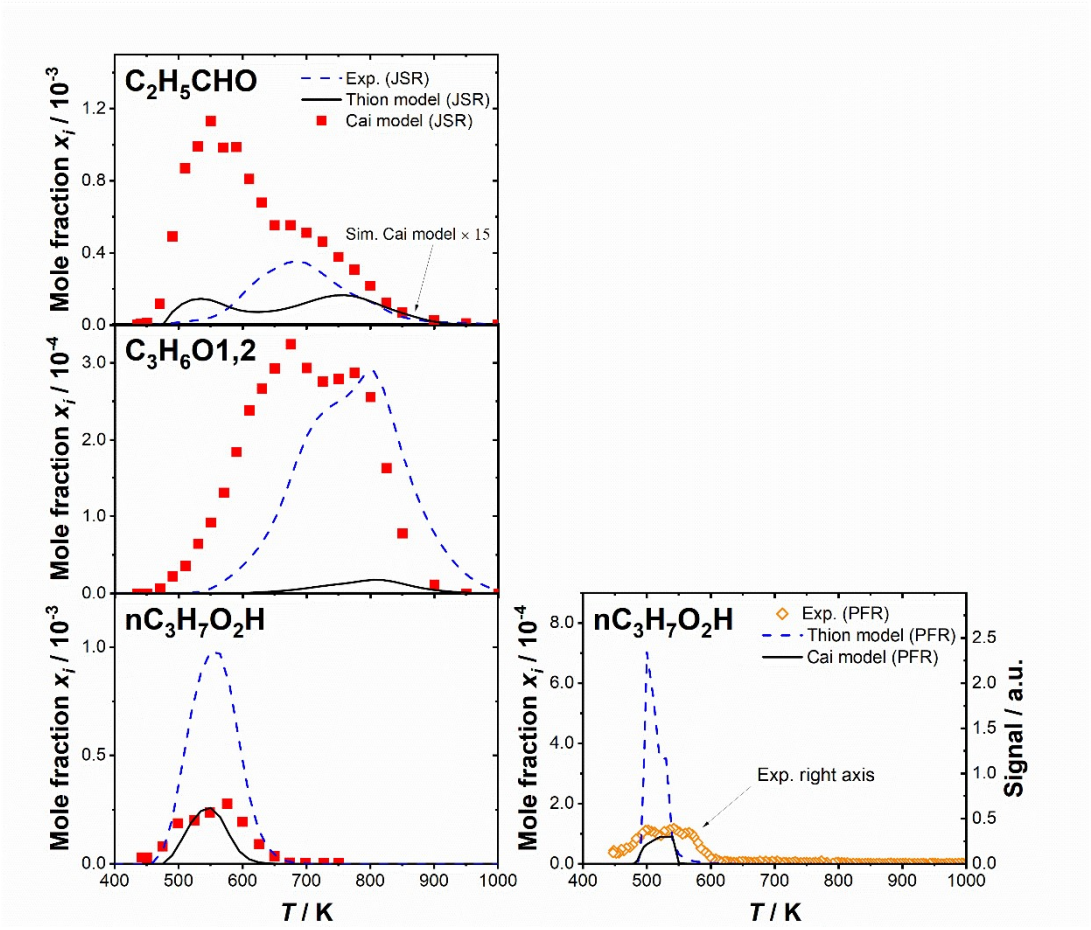

Fig. S11. Comparison of the experimental data and the Thion [1] and Cai [2] model for additional C_3 intermediate species. **Left panel:** JSR. **Right panel:** PFR.

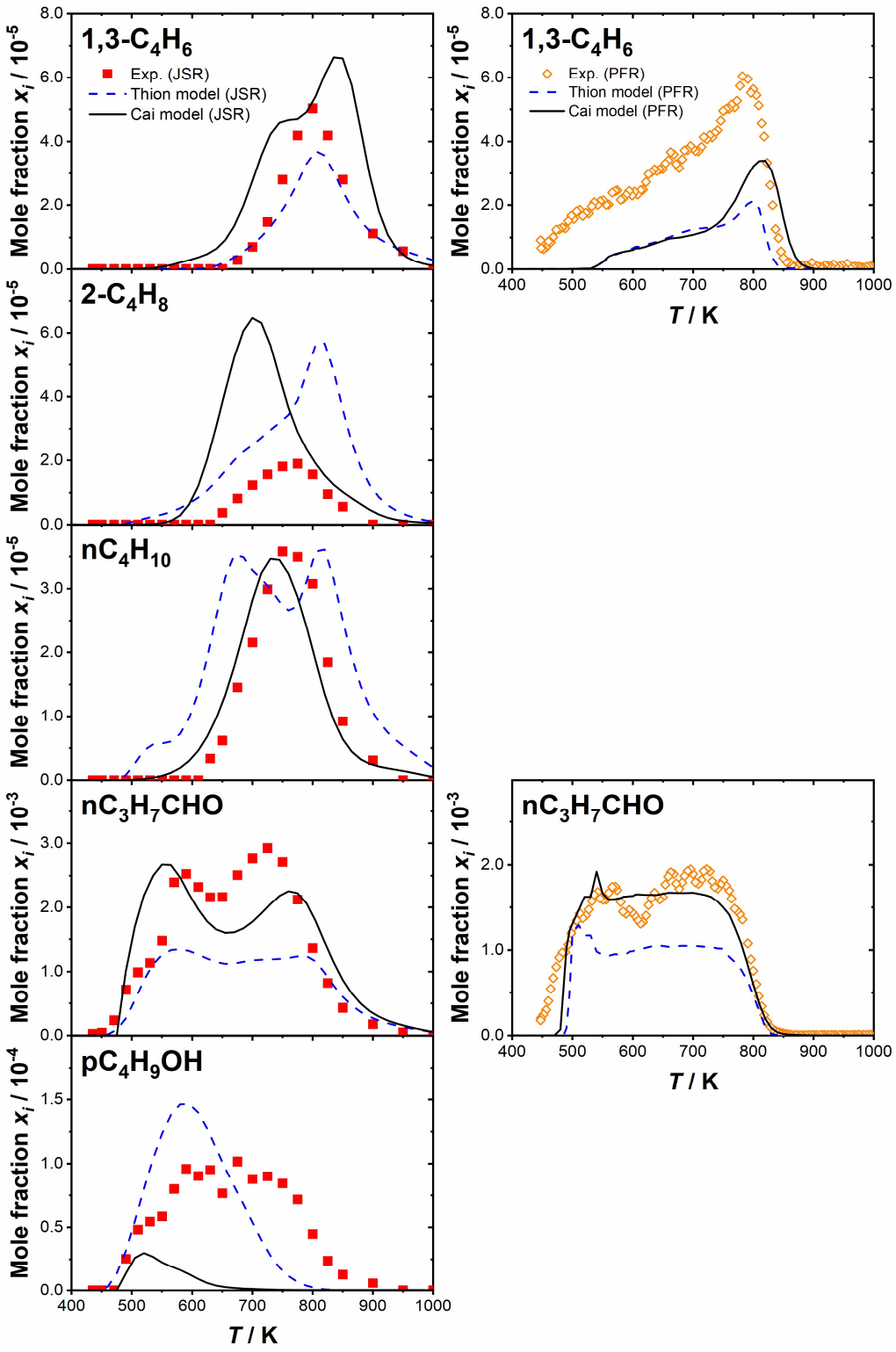

Fig. S12. Comparison of the experimental data and the Thion [1] and Cai [2] model for the selected C_4 intermediate species. **Left panel:** JSR. **Right panel:** PFR.

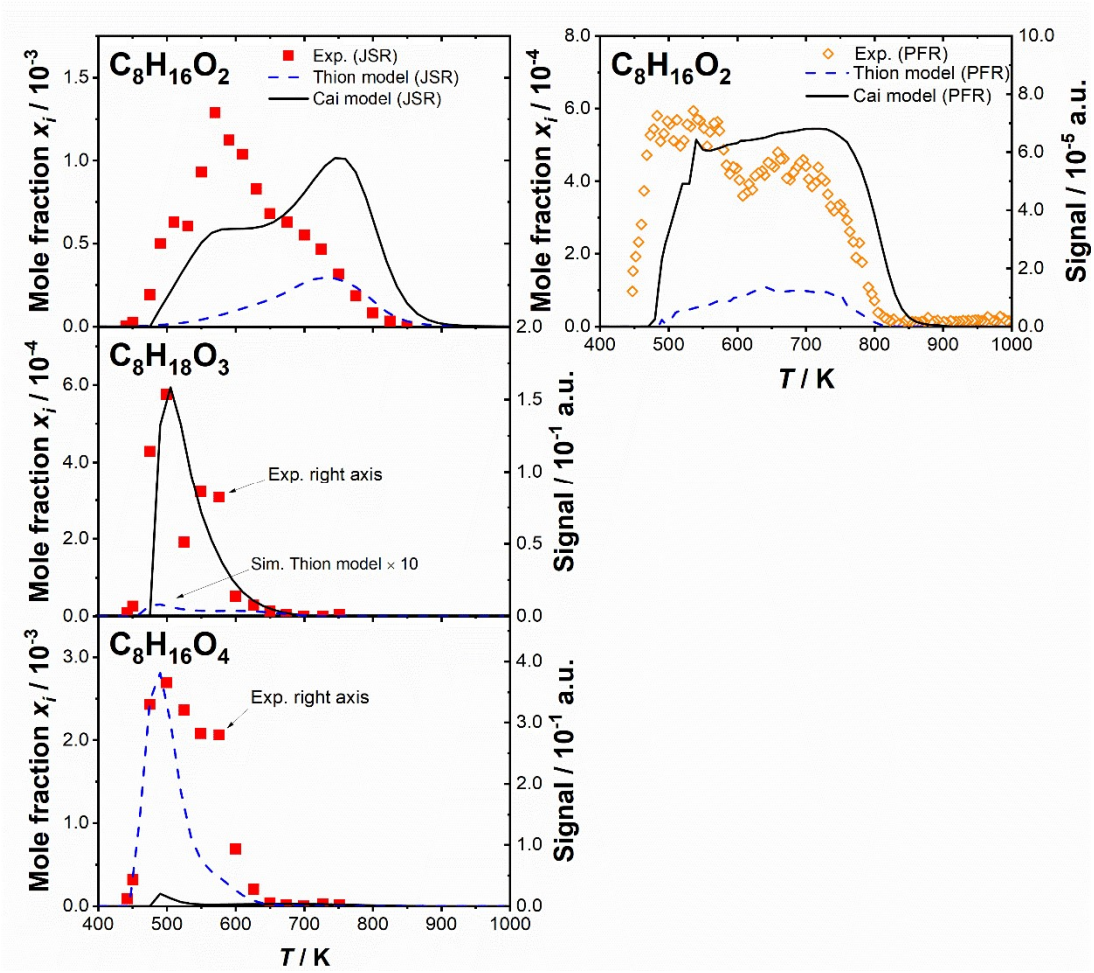

Fig. S13. Comparison of the experimental data and the Thion [1] and Cai [2] model for selected C_8 intermediate species. Both experimental and simulated results of $C_8H_{16}O_2$ represent sums of isomers. **Left panel:** JSR. **Right panel:** PFR.

References

[1] S. Thion, C. Togbé, Z. Serinyel, G. Dayma, P. Dagaut, A chemical kinetic study of the oxidation of dibutyl-ether in a jet-stirred reactor, Combust. Flame 185 (2017) 4–15.

[2] L. Cai, Y. Uygun, C. Togbé, H. Pitsch, H. Olivier, P. Dagaut, S.M. Sarathy, An experimental and modeling study of n-octanol combustion, Proc. Combust. Inst. 35 (2015) 419–427.